The metastable phase diagram and the kinetics of transient ordered states in a ternary system

1998 J. Phys.: Condens. Matter 10 3523

(http://iopscience.iop.org/0953-8984/10/16/006)

J. Phys.: Condens. Matter **10** (1998) 3523–3534. Printed in the UK PII: S0953-8984(98)87881-8

The metastable phase diagram and the kinetics of transient ordered states in a ternary system

Jun Ni and Binglin Gu

Department of Physics, Tsinghua University, Beijing 100084, People's Republic of China

Received 25 September 1997, in final form 7 January 1998

Abstract. The kinetics of a ternary system is investigated using the cluster-variation method and the path probability method in the pair approximation. It is shown that differences between the diffusive jump rates for the three atomic species of a ternary system have a strong effect on the kinetics of the system. The calculated metastable phase diagram of the system shows the existence of transient ordered states during the relaxation both from the completely disordered state to the equilibrium disordered state and from the completely disordered state to the equilibrium ordered state due to the differences between the relaxation times for the three atomic species. The kinetic paths of ordering and disordering are classified according to the metastable phase diagram. From the study of the kinetics of ordering and disordering, it is shown that there are two types of transient ordered state and that there are overshooting effects during the relaxation from the disordered state to the equilibrium ordered state. It is also shown that there is an anomalous effect in the evolution of long-range ordering parameters in the kinetics of disordering for a ternary system.

1. Introduction

Non-equilibrium kinetics of materials plays an important role in materials growth. In recent years, new experimental methods such as rapid quenching, laser processing, ion-beam bombardment and various epitaxial processes have been used to prepare materials that are in non-equilibrium states thermodynamically. Equilibrium phase diagrams do not deliver sufficient information for such non-equilibrium growth processes. In order to obtain a better understanding of non-equilibrium growth processes, it is important to investigate the metastable phase diagrams and the fundamental aspects of the kinetics of ordering and disordering of the systems. In the kinetics of order–disorder transformations [1–5], there are two usual processes. One process is that in which a disordered phase develops into an ordered phase and the other is the process in which an ordered phase relaxes to an equilibrium disordered phase. It was found that there are various aspects to the kinetics of the ordering and disordering. In some systems, transient ordered states are formed during the relaxation from the non-equilibrium state to the equilibrium state [6–8]. For binary alloys, the occurrence of transient ordered states needs special conditions such as suitable interaction energy of the constituent atoms. For ternary alloys, the kinetic paths are less intuitive than for binary alloys [3]. In a binary alloy, there are only two species. Although there are two characteristic times for the atomic migration of the two species (A and B), only the time constant of the A–B atom exchange is responsible for the change of the structure of the system. Thus the kinetic relaxation time is determined by the slower of the diffusion rates of the two species for a binary system. In a ternary system, there are

0953-8984/98/163523+12$19.50

more characteristic times for the atomic migration that control the relaxation of different species and thus significant differences in the kinetics can arise correspondingly. Due to the differences in the characteristic times for the atomic migration of the three species in a ternary system, two of the three species may first form a kind of transient state on its relaxation path to the final equilibrium phase. In this paper, we will investigate the formation and kinetics of the transient states in a ternary system. We will show that there is a type of transient ordered state in the ternary system due to the differences in the diffusion rates of the three atomic species from the calculated metastable phase diagram. The kinetic paths of ordering and disordering are classified according to the metastable phase diagram. Different types of evolution process are calculated and analysed. Several features in the kinetics of the ordering and disordering are illustrated

The outline of this paper is as follows. Section 2 presents the results on the metastable phase diagram. Section 3 describes the kinetics of the transient states. In section 4 we give our conclusions.

2. The metastable phase diagram

We describe a ternary system $A_xB_yC_{1-x-y}$ as a lattice gas with the Hamiltonian

$$\mathcal{H} = \sum_{\{ij\}} \sum_{ss'} E_{ss'} c_i^s c_j^{s'} - N \sum_s \mu_s x_s. \tag{1}$$

The variable $c_i^s = 1$ if the site i is occupied by an atom s (=A, B, C) and is zero otherwise. The notation $\{ij\}$ means summation over the pairs of nearest-neighbour lattice sites. $E_{ss'}$ represents the nearest-neighbour interaction energy. N is the number of lattice sites, μ_s is the chemical potential and x_s is the concentration of the s-species. In the following, we will use the subscripts 1, 2, 3 to represent the A, B, C species of atoms respectively.

We can also use the three-component Blume–Emery–Griffiths (BEG) spin model [9, 10] to represent the Hamiltonian of a ternary system equivalently, by mapping the spin $s_i = \{+1, -1, 0\}$ onto the species A, B and C:

$$\mathcal{H} = J \sum_{\{i,j\}} s_i s_j - K \sum_{\{i,j\}} s_i^2 s_j^2 + L \sum_{\{i,j\}} (s_i^2 s_j + s_i s_j^2) + \mu \sum_i s_i^2 + h \sum_i s_i. \tag{2}$$

The energy parameters of the BEG Hamiltonian are related to the atomic nearest-neighbour interaction energies in the alloy Hamiltonian by the following equations [10]:

$$4J = E_{11} + E_{22} - 2E_{12} \tag{3}$$

$$4K = -E_{11} - E_{22} - 2E_{12} - 4E_{33} + 4(E_{13} + E_{23}) \tag{4}$$

$$4L = E_{11} - E_{22} + 2(E_{23} - E_{13}) \tag{5}$$

$$\mu = \mu_3 - \frac{1}{2}(\mu_1 + \mu_2) - zE_{33} + \frac{z}{2}(E_{13} + E_{23}) \tag{6}$$

$$h = \frac{1}{2}(\mu_2 - \mu_1) - \frac{z}{2}(E_{23} - E_{13}) \tag{7}$$

where z is the coordination number of the lattice. Since the alloy Hamiltonian of equation (1) and the BEG Hamiltonian of equation (2) are equivalent, only three independent energy parameters, such as J, K, L, are required to describe the equilibrium phase diagram. This point will be made clearer if we compare with the binary system. For a binary system, only one energy parameter $\epsilon = E_{12} - (E_{11} + E_{22})/2$ is relevant to the phase diagram. The three species of a ternary system can form three combinations of binary systems. So we have three energy parameters to describe the phase diagram in a ternary

system. There are six independent nearest-neighbour interaction energies in the lattice-gas Hamiltonian (1). Due to the constraint $c_i^A + c_i^B + c_i^C = 1$, not all of the terms appearing in (1) are 'interaction' terms. Taking, e.g., $c_i^C = 1 - c_i^A + c_i^B$, the energy term in the lattice-gas Hamiltonian may be rewritten in terms of A and B variables. There are three 'interaction' terms $E'_{AA} = E_{AA} - 2E_{AC} + E_{CC}$, $E'_{AB} = E_{AB} - E_{AC} - E_{BC} + E_{CC}$ and $E'_{BB} = E_{BB} - 2E_{BC} + E_{CC}$, two 'local potential' terms ϵ_A and ϵ_B, and a constant term $E_0 = NzE_{CC}/2$. The 'local potential' terms can be added to the chemical potential terms. At fixed concentrations x_1 and x_2, the Helmholtz free energy $F = F_{int} + F_{loc}$ is such that the 'local potential' contribution is trivially $F_{loc} = N(\epsilon_A x_1 + \epsilon_B x_2) + E_0$, which is the same for all of the phases, so the equilibrium properties are determined by only three parameters (e.g. J, K, L) by just comparing the 'interaction' contribution F_{int} in the different phases.

The spin-1 BEG model is a model which was originally used to describe the phase transition in ^{3}He–^{4}He mixtures [9]. It has been shown that the BEG model has rich structures in the phase diagrams [11–17]. In order to compare with the equilibrium properties, we use the cluster-variation method [18–21] in the pair approximation, which is also often called the Bethe–Peierls approximation, to calculate the equilibrium phase diagram. In the pair approximation, the oriented-pair probability that an s-atom on an α-sublattice site is bonded to an s'-atom on a β-sublattice site is represented by $P_{ss'}$ and the probability that an s-atom occupies an α-sublattice site is represented by P_s^α. The equilibrium state of the system is derived by minimizing the grand-canonical potential G defined as

$$G = E - TS - N\sum_{i=1}^{3}\mu_i x_i \tag{8}$$

where T is the absolute temperature. E is the energy of the alloy given by

$$E = zN\sum_{i,j} E_{i,j}P_{ij}. \tag{9}$$

S is the configurational entropy given by

$$S = Nk_B\left[-z\sum_{i,j} P_{ij}\ln P_{ij} + (z-1)\sum_{i,\nu} P_i^\nu \ln P_i^\nu\right] \tag{10}$$

where k_B is Boltzmann's constant.

The symmetry of the phase in the system is determined by the site probability P_s^ν. For the situation in which it is possible to subdivide the lattice into two sublattices α and β, we can also describe the phase in terms of the magnetization and quadrupolar moments of the sublattices α and β in the BEG model:

$$m_\alpha = \langle s_i\rangle_\alpha \qquad m_\beta = \langle s_i\rangle_\beta \qquad q_\alpha = \langle s_i^2\rangle_\alpha \qquad q_\beta = \langle s_i^2\rangle_\beta. \tag{11}$$

The values of these parameters define the following phases with different symmetries:

(1) the disordered phase: $m_\alpha = m_\beta$, $q_\alpha = q_\beta$;
(2) the ordered phase O_1: $m_i \neq 0$, $m_\alpha \neq m_\beta$;
(3) the ordered phase O_2: $m_\alpha = 0$ or $m_\beta = 0$, $q_\alpha \neq q_\beta$.

For the determination of the phase diagrams of the system, we minimize the grand potential G using the Kikuchi natural iteration scheme [19] in which the chemical potentials μ_i and temperature T are the input variables. As we change the chemical potential μ and temperature T, we can determine the phase boundaries by searching for those special values of the chemical potentials μ_i and corresponding compositions x_i for which two phases coexist.

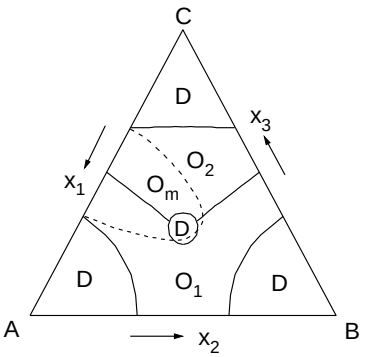

Figure 1. The calculated equilibrium phase diagram (solid line) and metastable phase diagram (dotted line) at $k_BT = 0.1$ eV in the Gibbs composition triangle. O_1 and O_2 are two ordered phases in the equilibrium phase diagram and O_m is the ordered phase in the metastable phase diagram. The disordered phase is indicated as D.

We will investigate the case in which it is possible to subdivide the lattice into two sublattices α and β. The honeycomb lattice is one of the simplest lattices with two sublattices. For the BEG model on the honeycomb lattice, extensive studies have been carried out by different techniques and this has provided the basis for the investigations on the kinetics of the system. The BEG model on the honeycomb lattice has been solved exactly for some subspaces in the energy parameter space [22–26]. Kaneyoshi [27, 28] has studied the phase diagrams for the honeycomb lattice by means of the correlated-effective-field method (CEFT). Gwa and Wu [29] have determined the critical surface of second-order transitions of the BEG model on the honeycomb lattice. Rosengren and Lapinskas [17] have investigated the phase diagram of the BEG model on the honeycomb lattice using the CVM. There have also been investigations of the ternary system on the honeycomb lattice using an alloy Hamiltonian which is equivalent to the BEG model via the CVM [4] and Monte Carlo method [30]. Smith and Zangwill [4] have calculated the equilibrium phase diagrams and the kinetics of the ordering and disordering on the two-dimensional honeycomb lattice. They have only considered the case in which the diffusion rates of all of the atomic species are the same. Since we will investigate how the differences in the diffusion rates of the three atomic species affect the kinetics of the system, we will consider the two-dimensional honeycomb lattice as a representative case in the following and compare our results with those of Smith and Zangwill [4] and Monte Carlo results for the same lattice and same energy parameters. The results for the square lattice are similar. We choose the same interaction energies as were used by Smith and Zangwill [4] and Zhang and Murch [30], e.g., $E_{11} = E_{22} = 1.0$ eV, $E_{12} = 0.8$ eV and $E_{13} = E_{23} = E_{33} = 0.0$ which correspond to the energy parameters $J = 0.1$ eV, $K = -0.9$ eV, $L = 0.0$. A system with such energy parameters exhibits ordering for all three species because the alloy parameters $\epsilon_1 = E_{12} - (E_{11} + E_{22})/2 < 0$, $\epsilon_2 = E_{13} - (E_{11} + E_{33})/2 < 0$ and $\epsilon_3 = E_{23} - (E_{22} + E_{33})/2 < 0$. A system with such energy parameters is expected to exhibit no phase separation. Figure 1 shows the calculated equilibrium phase diagram of the ternary system at $T = 0.1$ eV in the Gibbs composition triangle. In the phase diagram, there are two ordered phases, O_1 and O_2. In the ordered phase O_1, component C has a disordered distribution and the ordering occurs among the A and B atoms, which reflects the usual binary ordering scenario of A and B atoms. In the ordered phase O_2, the ordering occurs among components C and A + B. Between the ordered phase O_1 and the ordered phase O_2, there is a hole-shaped disordered region in the

middle of the triangle. The results are similar to those from the previous calculations for equilibrium phase diagrams [4, 30]

Now we consider the calculation of the metastable phase diagram of the system. Two factors affect the kinetics of the system in the relaxation of the system from a non-equilibrium state to an equilibrium state: (i) the atomic interaction energy; and (ii) the activation barrier height which determines the diffusive jumping rates of the atoms. Generally the activation barrier energies of A and B atoms are different. In order to investigate how these different activation barrier energies and correspondingly the different diffusive jumping rates of the atoms affect the kinetics of the system, we consider an extreme case, i.e. that in which one species (taken as A atoms) moves much more slowly than the other two species (taken as B and C atoms). The initial state of the system is chosen to be a completely disordered state, which would correspond to the configuration of a system quenched from high temperature. The system will relax to its equilibrium state in two stages. In the first stage, only B and C atoms move while A atoms are in a state of relative rest because A atoms move much more slowly than B and C atoms. The system evolves to a metastable state in which A atoms remain in their disordered configuration and B and C atoms have relaxed to their local equilibrium state. After the system reaches the metastable state, the evolution process enters its second stage. In the second stage, A atoms slowly move and the whole system relaxes to its final equilibrium state gradually.

In the calculation of the metastable phase diagram, we use the modified Kikuchi approximation [31] in order to study the metastable phase. The Helmholtz free energy $F = E - TS$ is minimized instead of the grand-canonical potential. Since A atoms are randomly distributed in the metastable state, there are three constraint equations that represent the random distribution of A atoms:

$$\sum_i P_{1i} = x_1 \qquad \sum_i P_{i1} = x_1 \qquad P_{11} = x_1^2. \tag{12}$$

We use undetermined Lagrange multipliers to treat the constraints. For each Kikuchi natural iteration we use the method of steepest descent to determine the undetermined Lagrange multipliers. The dotted line in figure 1 shows the calculated metastable phase diagram. It is interesting to note that the ordered phase region of the metastable phase diagram is not all included in the ordered phase region of the equilibrium phase diagram. Some of the metastable ordered phase region overlaps with the equilibrium disordered phase region. This means that a transient ordered phase O_m will occur in the first stage of the kinetic evolution of a highly disordered phase in the overlap region if A atoms move much more slowly. Since the equilibrium phase of this overlap region is a disordered phase, this transient ordered phase will evolve to an equilibrium disordered phase finally. Therefore its kinetic route is expected to be disordered state–ordered state–disordered state. From figure 1 it can be seen that the region of the metastable phase O_m also overlaps with that of the ordered phases O_1 and O_2. In the regions of overlap of the metastable phase O_m and the ordered phases O_1 and O_2, we also expect a transient ordered state characteristic of O_m to occur during the relaxation from the initial disordered phase to the ordered phases O_1 and O_2 if A atoms move more slowly. Thus the kinetic paths can be classified according to the metastable phase diagram.

3. The kinetics of transient states

We employ the path probability method (PPM) [1, 2, 32] to investigate the non-equilibrium evolution process of the system. The path probability method can be shown to be equivalent

[33] to the master equation method (MEM) [34] in the pair approximation. In the kinetic process, there are two atom movement mechanisms: (i) the direct interchange of an atom with a nearest-neighbour atom (the atom–atom interchange mechanism); and (ii) the interchange of an atom with an adjacent vacancy (the vacancy mechanism). A general case will combine both two-atom movement mechanisms. We consider a representative kinetic mechanism which allows only interchanges between (a) components A and C and (b) components B and C. This mechanism is used in the following two systems: (i) a conventional ternary alloy with a direct atom interchange mechanism, with the condition that A–B atom interchange is much slower than other atom interchanges; and (ii) a quasi-ternary system with two atomic constituents and one vacancy component, with an atom–vacancy interchange mechanism. We are concerned with the case of the full range of vacancy concentration which can describe the ordering and disordering of co-deposition of a monolayer composed of two atomic constituents onto a crystal surface [4] rather than the kinetics of bulk binary alloys mediated by a very small vacancy concentration. Other kinetic mechanisms can lead to quantitative differences in the kinetics of the system, but the qualitative features will remain similar.

There are six independent pair probabilities which are characterized by three long-range order (LRO) parameters

$$\gamma_1 = P_1^{\alpha} - P_1^{\beta} \qquad \gamma_2 = P_2^{\alpha} - P_2^{\beta} \qquad \gamma_3 = P_{13} - P_{31} \tag{13}$$

and three short-range order (SRO) parameters

$$\gamma_4 = P_{13} + P_{31} \qquad \gamma_5 = P_{23} + P_{32} \qquad \gamma_6 = P_{12} + P_{21}. \tag{14}$$

The signs of the LRO parameters γ_1 and γ_2 are opposite in the ordered phase O_1. In the phase O_2, these LRO parameters have the same sign. In the disordered phase all of the LRO parameters are zero.

We determine the time evolution of the LRO and SRO by use of the PPM. In the PPM, the path probability function is defined as the counterpart of the free-energy functional of the CVM. There are two types of path variable, $X_{i,j}^{\nu}(t, t + \Delta t)$ and $Y_{ij,i'j'}(t, t + \Delta t)$, in the pair approximation used to describe the path probability. The superscript ν $(=\alpha, \beta)$ denotes the sublattices of the site probability. $X_{i,j}^{\nu}(t, t + \Delta t)$ describes the fraction of the species which are i at time t and will change to i' at $t + \Delta t$, and $Y_{ij,i'j'}(t, t + \Delta t)$ is the fraction of pairs which are (i, j) at time t and will change to (i', j') at $t + \Delta t$. The path probability function P is given as the product of three terms. The first one corresponds to the probability of occurrence of the unit kinetic process:

$$P_1 = \prod_{\nu} \prod_{i=1}^{2} (\theta_i \, \Delta t)^{NX_{i,3}^{\nu} + NX_{3,i}^{\nu}} (1 - \theta_i \, \Delta t)^{NX_{i,i}^{\nu} + NX_{3,3}^{\nu}} \tag{15}$$

where θ_1 is the rate of atomic exchange between species A and C, and θ_2 is the rate of atomic exchange between species B and C. θ_i is temperature dependent for a thermal activation process overcoming the saddle point energy of an exchange event. The second factor depends on the activation energy and is a generalization of the Boltzmann factor. With the use of the energy change in Δt of the system:

$$\Delta E = \sum_{i,j} E_{i,j} [P_{i,j}(t + \Delta t) - P_{i,j}(t)] \tag{16}$$

the second factor is taken to be

$$P_2 = \exp\left(-\frac{\Delta E}{2k_B T}\right). \tag{17}$$

The third factor is the combinatorial factor corresponding to the entropy in the equilibrium case. The state variables in the combinatorial factor of the CVM are replaced by the path variables in the corresponding approximation:

$$P_3 = \left(\prod_{\nu}\prod_{i,j}(NX_{i,j}^{\nu})!\right)^{z-1} \Bigg/ \left[\left(\prod_{(i,j)(i',j')}(NY_{ij,i'j'})!\right)^{z}(N!)^{z-2}\right]. \tag{18}$$

Thus the first term, P_1, gives the contribution to the path probability function from non-correlated atomic jumps whereas the second term, P_2, represents the thermally activated process. The key feature of the PPM is provided by the last term, P_3, which represents the number of possible paths from one given configuration to another. The path variables $Y_{ij,kl}$ can be represented by the path variables $Y_{i3,3i}$ and $Y_{3i,i3}$. We obtain the most probable path variables by differentiating $P(t, t+\Delta t)$ with respect to the independent path variables $Y_{i3,3i}$ and $Y_{3i,i3}$.

This leads to a set of six coupled non-linear differential equations, which have the form

$$\frac{\mathrm{d}}{\mathrm{d}t}\gamma_i(t) = f_i(\tau_1, \tau_2, \gamma_1, \gamma_2, \gamma_3, \gamma_4, \gamma_5, \gamma_6) \tag{19}$$

where

$$\tau_1 = \theta_1^{-1}\exp\left(-\frac{z(E_{13}-E_{33})}{k_BT}\right) \tag{20}$$

$$\tau_2 = \theta_2^{-1}\exp\left(-\frac{z(E_{23}-E_{33})}{k_BT}\right). \tag{21}$$

τ_1 and τ_2 are the characteristic times for the relaxation of A and B atoms respectively. When E_{13}, E_{23} and E_{33} are taken to be zero, $\tau_1 = \theta_1^{-1}$ and $\tau_2 = \theta_2^{-1}$. Because τ_1 and τ_2 depend on E_{13}, E_{23} and E_{33}, τ_1 and τ_2 could be very different even in the case where $\theta_1^{-1} = \theta_2^{-1}$ if E_{13} and E_{23} are very different. Due to the equivalence between the alloy Hamiltonian equation (1) and the BEG Hamiltonian equation (2), different sets of E_{ij} with same J, K, L lead to the same equilibrium phase diagram. Therefore, the interaction energy E_{ij} affects the kinetics of the system only through the energy parameters J, K, L and the characteristic times τ_1 and τ_2.

We have performed a calculation of the kinetics of the system for different τ_1 and τ_2. The different types of kinetic path classified according to the metastable phase diagram in figure 1 are considered. The differential equations describing the kinetics of the system were integrated numerically using Gear's method [35], appropriate to stiff differential equations. The equilibrium values obtained from the kinetic equations at sufficiently long time reproduced those obtained from the equilibrium phase diagram calculation.

First we consider the kinetics of ordering. The initial state is chosen as a completely random state which can be obtained by quenching the system from high temperature. Thus the initial values of the SRO parameters are those characteristic of a completely random state. The LRO parameters are set to 10^{-6} at $t = 0$ to describe the incipient fluctuation. Figure 2 illustrates the evolution of the LRO parameter at a typical point in the overlap region of the metastable ordered phase O_m and the equilibrium disordered phase in the phase diagram of figure 1. We have taken $\tau_1/\tau_2 = 10^3$. There are two types of transient ordered state. One (denoted by the symbol O_{t1}) has the characteristics of the metastable phase O_m in the metastable phase diagram of figure 1. The other (denoted by the symbol O_{t2}) has the characteristics of O_1 because the signs of its LRO parameters γ_1 and γ_2 are opposite. This shows that the kinetics of the system is more complicated than that obtained simply from the analysis of the metastable phase diagram. The system first evolves to the

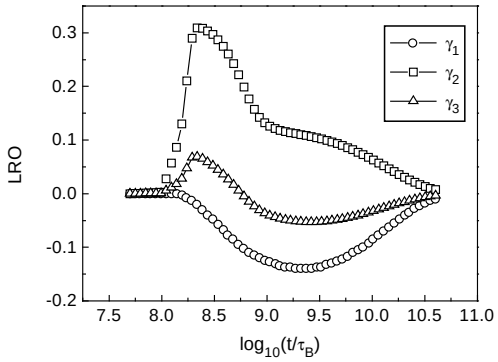

Figure 2. The evolution of the LRO at a typical point in the overlap region of the equilibrium disordered phase and the metastable ordered phase O_m, with the concentrations of the three species set at $x_1 = 0.34$, $x_2 = 0.36$ and $x_3 = 0.3$. $k_BT = 0.1$ eV and $\tau_1/\tau_2 = 10^3$.

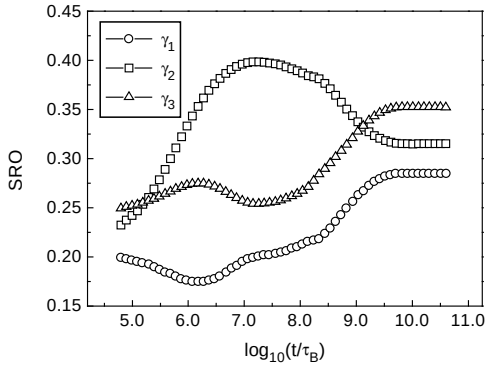

Figure 3. The evolution of the SRO at a typical point in the overlap region of the equilibrium disordered phase and the metastable ordered phase O_m, with the concentrations $x_1 = 0.34$, $x_2 = 0.36$ and $x_3 = 0.3$. $k_BT = 0.1$ eV and $\tau_1/\tau_2 = 10^3$.

transient ordered state O_{t1} with the characteristics of O_m, in which γ_1 is zero and A atoms remain disordered. Then the magnitude of γ_1 increases gradually, while γ_2 decreases and γ_3 changes from positive to negative. The system evolves to the transient ordered state O_{t2}. Finally, all of the LRO parameters become zero. We could consider the kinetics in the overlap region as a competition between O_1 and O_2, since it is in the V-shaped region between O_1 and O_2. Figure 3 shows the evolution of the SRO with the same parameters as those of figure 2. From the timescale in the figure, we can see that all of the SRO parameters change very rapidly. There are several stages in the change. The parameters first develop from the values of the completely disordered state into those of the correlated state with short-range order until the system begins to develop into the transient phase O_{t1}. Then the SRO parameters evolve to the quasi-equilibrium values of the transient phase O_{t1} and then those of O_{t2}. Finally, all of the SRO parameters develop to their equilibrium values, and then remain almost constant during the time period over which the LRO decays to the zero value of its final equilibrium disordered phase. This final stage of the kinetics shows that the system is driven to its equilibrium disordered state by entropy alone, since the SRO parameters change very little; this is also characteristic of other disordering kinetics [2–4].

Figure 4 shows the evolution of the LRO in the overlap region of the metastable ordered

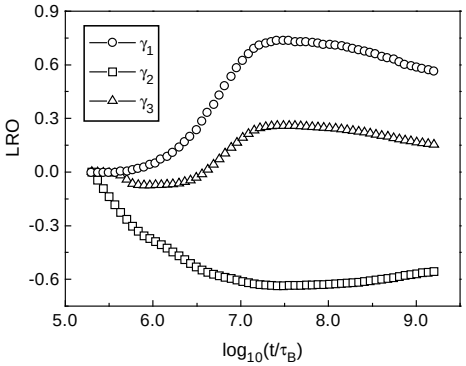

Figure 4. The evolution of the LRO at a typical point in the overlap region of the equilibrium ordered phase O_1 and the metastable ordered phase O_m, with the concentrations of the three species set at $x_1 = 0.37$, $x_2 = 0.37$ and $x_3 = 0.26$. $k_BT = 0.06$ eV and $\tau_1/\tau_2 = 10^4$.

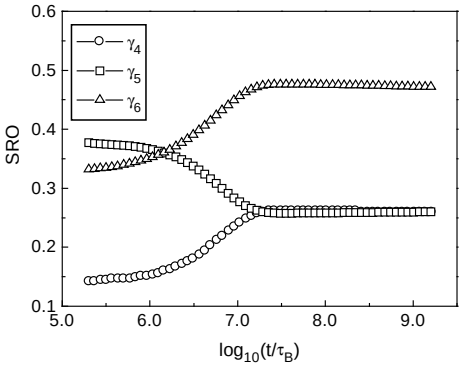

Figure 5. The evolution of the SRO at a typical point in the overlap region of the equilibrium ordered phase O_1 and the metastable ordered phase O_m, with the concentrations $x_1 = 0.37$, $x_2 = 0.37$ and $x_3 = 0.26$. $k_BT = 0.06$ eV and $\tau_1/\tau_2 = 10^4$.

phase O_m and the equilibrium ordered phase O_1 in the phase diagram of figure 1. We have taken $\tau_1/\tau_2 = 10^4$. We can see that there are two stages of the relaxation. In the first stage, the system evolves to the transient ordered state O_{t1}. Then the system relaxes to its equilibrium ordered phase O_1. It is interesting to note that the system does not approach the equilibrium ordered phase monotonically. There is a peak in the relaxation curves of the LRO parameters γ_1 and γ_2, which means that there is an overshooting effect in the evolution of the system. This effect has also been found in the kinetics of ordering and disordering for other systems [36, 37]. Figure 5 illustrates the evolution of the corresponding SRO which shows clearly that there is a transformation from the SRO of the transient ordered phase O_{t1} to that of the equilibrium ordered phase O_1. The SRO relaxes much more quickly than the LRO, which is reflected by the flat plateau in the curves of the SRO.

Figure 6 shows the evolution of the LRO in the overlap region of the metastable ordered phase O_m and the equilibrium ordered phase O_2 in the phase diagram of figure 1. The figure shows the two relaxation stages clearly. The system first evolves into the transient ordered state O_{t1} and then relaxes into its equilibrium ordered phase O_2. In both stages of the evolution, there are substantial overshooting effects in the LRO parameters γ_2. There is also an overshooting for γ_3 in the evolution from the disordered phase to the transient

ordered phase O_{t1}. But in the late stage, there is no overshooting for γ_3. Figure 7 illustrates the evolution of the corresponding SRO.

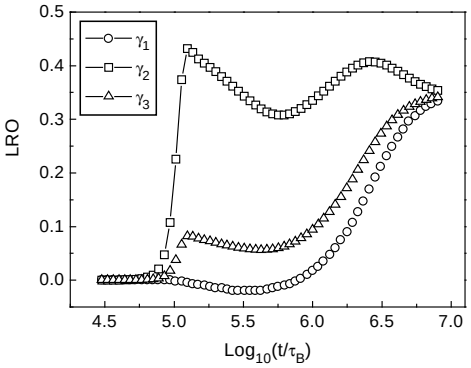

Figure 6. The evolution of the LRO at a typical point in the overlap region of the equilibrium ordered phase O_2 and the metastable ordered phase O_m, with the concentrations of the three species set at $x_1 = 0.3$, $x_2 = 0.3$ and $x_3 = 0.4$. $k_BT = 0.1$ eV and $\tau_1/\tau_2 = 10^3$.

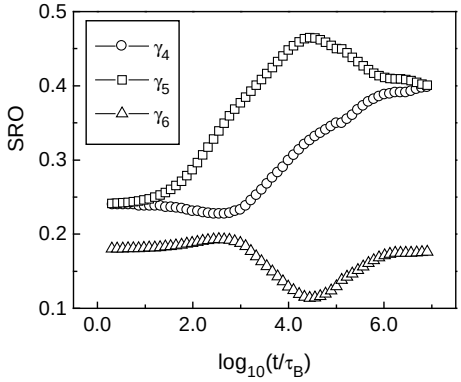

Figure 7. The evolution of the SRO at a typical point in the overlap region of the equilibrium ordered phase O_2 and the metastable ordered phase O_m, with the concentrations of the three species set at $x_1 = 0.3$, $x_2 = 0.3$ and $x_3 = 0.4$. $k_BT = 0.1$ eV and $\tau_1/\tau_2 = 10^3$.

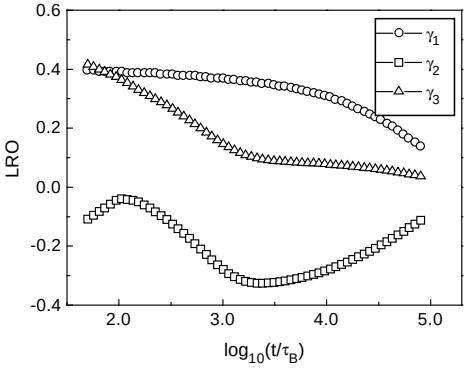

Figure 8. The evolution of the LRO in the region of the equilibrium disordered phase, with the concentrations of the three species set at $x_1 = 0.4$, $x_2 = 0.4$ and $x_3 = 0.2$. $k_BT = 0.2$ eV and $\tau_1/\tau_2 = 10^2$.

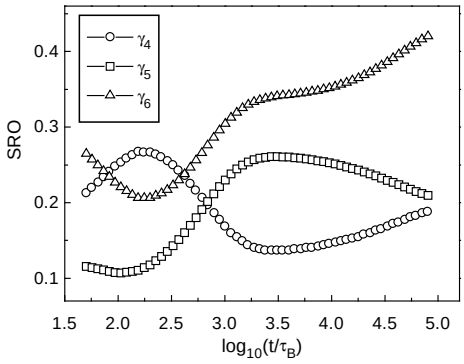

Figure 9. The evolution of the SRO in the region of the equilibrium disordered phase, with the concentrations of the three species set at $x_1 = 0.4$, $x_2 = 0.4$ and $x_3 = 0.2$. $k_BT = 0.2$ eV and $\tau_1/\tau_2 = 10^2$.

We have also studied the kinetics of disordering. The initial state of the system is chosen as the ordered state for low temperature which has the maximal LRO and SRO. Figure 8 shows the evolution of the LRO. The composition of the system is chosen as: $x_1 = 0.4$, $x_2 = 0.4$ and $x_3 = 0.2$. The system is relaxed at $k_BT = 0.2$ eV. It can be seen that the LRO parameter γ_1 decays monotonically while the variation of γ_2 shows fluctuation. γ_2 decays to zero initially. But with the movement of A atoms, there is an inverse process in which γ_2 increases anomalously. After reaching a maximum, at which a bending on the evolution curve of γ_3 also occurs concurrently, γ_2 eventually decays to zero. Figure 9 shows the evolution of the corresponding SRO. It shows clearly that the different evolution aspects of the LRO at the different times in figure 8 are largely due to the differences in the corresponding SRO of the system. The differences in the relaxation times are responsible

for the deviation of the evolution curve of the LRO and SRO from monotonic decay.

We have also investigated how the kinetics of the system changes with the ratio τ_1/τ_2. Smith and Zangwill [4] have studied the kinetics of ordering and disordering on a two-dimensional honeycomb lattice by the master equation method. They only considered the case where $\tau_1/\tau_2 = 1$, which shows no transient state. In our study, we find that when $\tau_1/\tau_2 = 1$, the initial completely random state will relax to the equilibrium state directly. With the increase of the ratio τ_1/τ_2, we find that the ordering parameters of the transient ordered state increase gradually. Therefore the ratio τ_1/τ_2 which measures the difference of the two characteristic times in the ternary system determines the occurrence of the transient ordered state O_{t1}.

4. Conclusions

We have investigated the kinetics of a ternary system. From the calculated metastable phase diagram, we have predicted the occurrence of a transient ordered state in the kinetic process of the system in the region of the metastable phase O_m if one of the three components has a slower relaxation time. Since the calculation of the metastable phase diagram is unrelated to the specific kinetic mechanism, the occurrence of the ordered state O_m in the kinetics of the system does not depend on the specific kinetic mechanism. By means of the metastable phase diagrams associated with the differences in the diffusion rates of the three atomic species, we can characterize the kinetic path to equilibrium with the metastable ordered state O_m.

We have calculated the evolution of the LRO and SRO using the PPM in the pair approximation. The different types of kinetic path classified according to the metastable phase diagram are considered. We find that there are two transient ordered states O_{t1} and O_{t2} in the relaxation from the completely disordered state to the equilibrium disordered state in the region of overlap between the equilibrium disordered state and the metastable ordered state. When we quench the transient ordered state O_{t1} or O_{t2} in the disordered region of the phase diagram, it is possible to preserve an ordered state at a temperature at which otherwise an equilibrium disordered phase should occur. It can also be seen that the SRO plays an important role in the kinetics of the transient states in the ternary system. If there is no SRO, there is only one type of disordered phase, i.e. there is a completely random state, the initial disordered phase will be same as the final equilibrium disordered phase and, thus, no transient state will occur. However, if there is SRO, the final equilibrium disordered phase with SRO will be different from the initial disordered phase. For the kinetics of ordering in the region of overlap between the metastable ordered state and the equilibrium ordered state, there is a transient ordered state O_{t1} and an overshooting effect during the relaxation from the completely disordered state to the equilibrium ordered state. We have also studied the kinetics of disordering and found that the LRO does not always decay to zero monotonically. There is an anomalous increase in the LRO parameters during the relaxation from the ordered state to the equilibrium disordered state when there are differences between the characteristic times measuring the migration rates of the atomic species in the ternary system. The differences in the diffusion rates of the three atomic species affect the migration of the atoms of the different species and change the SRO of the system. For the two points with roughly the same LRO on either side of the overshooting peak of the LRO, the corresponding SRO differs and this dictates the different evolution paths of the LRO; this is also the mechanism of the non-monotonic relaxation. Thus the differences in the diffusive jump rates for the different atomic species of a ternary system lead to a rich variety of features in the kinetics of ordering and disordering.

References

[1] Sato H and Kikuchi R 1976 *Acta Metall.* **24** 797
[2] Gschwend K, Sato H and Kikuchi R 1978 *J. Chem. Phys.* **69** 5006
[3] Fultz B 1992 *J. Mater. Res.* **7** 946
[4] Smith J R Jr and Zangwill A 1994 *Surf. Sci.* **316** 359
[5] Mohri T 1990 *Acta Metall.* **38** 2455
[6] Fultz B 1989 *J. Mater. Res.* **5** 1132
[7] Chen L Q and Khachaturyan A G 1991 *Phys. Rev.* B **44** 4681
[8] Reinhard L and Turchi P E A 1994 *Phys. Rev. Lett.* **72** 120
[9] Blume M, Emery V J and Griffiths R B 1971 *Phys. Rev.* A **4** 1071
[10] Mukamel D and Blume M 1974 *Phys. Rev.* A **10** 610
[11] Hoston W and Berker A N 1991 *Phys. Rev. Lett.* **67** 1027
[12] Hoston W and Berker A N 1991 *J. Appl. Phys.* **70** 6101
[13] Newman K E and Xiang X 1991 *Phys. Rev.* B **44** 4677
[14] Ni J and Iwata S 1995 *Phys. Rev.* B **52** 3214
[15] Netz R R 1992 *Europhys. Lett.* **17** 373
[16] Rosengren A and Lapinskas S 1993 *Phys. Rev. Lett.* **71** 165
[17] Rosengren A and Lapinskas S 1993 *Phys. Rev.* B **47** 2643
[18] Kikuchi R 1951 *Phys. Rev.* **81** 988
[19] Kikuchi R 1977 *Acta Metall.* **25** 195
[20] An G 1988 *J. Stat. Phys.* **52** 727
[21] Morita T 1990 *J. Stat. Phys.* **59** 819
[22] Horiguchi T 1986 *Phys. Lett.* **113A** 425
[23] Wu F Y 1986 *Phys. Lett.* **116A** 245
[24] Shankar H 1986 *Phys. Lett.* **117A** 365
[25] Wu X N and Wu F Y 1988 *J. Stat. Phys.* **50** 41
[26] Rosengren A and Häggkvist R 1989 *Phys. Rev. Lett.* **63** 660
[27] Kaneyoshi T 1990 *Physica* A **164** 730
[28] Kaneyoshi T 1991 *J. Magn. Magn. Mater.* **95** 157
[29] Gwa L H and Wu F Y 1991 *Phys. Rev.* B **43** 13 755
[30] Zhang L and Murch G E 1991 *Solid State Ion.* **47** 125
[31] Gu B L, Ni J and Zhu J L 1992 *Phys. Rev.* B **45** 4071
[32] See for example
Prog. Theor. Phys. Suppl. 1988 **115**
[33] Ishikawa T, Wada K, Sato H and Kikuchi R 1986 *Phys. Rev.* A **33** 4164
[34] Saito Y and Kubo R 1976 *J. Stat. Phys.* **15** 233
[35] Gear W C 1971 *Numerical Initial Value Problems in Ordinary Differential Equations* (Englewood Cliffs, NJ: Prentice-Hall)
[36] Gilhøj H, Jeppesen C and Mouritsen O G 1995 *Phys. Rev. Lett.* **75** 3305
[37] Gilhøj H, Jeppesen C and Mouritsen O G 1996 *Phys. Rev.* E **53** 5491